

ONLINE-TUNED MULTI-MODE RESONANT PIEZOELECTRIC SHUNT FOR BROADBAND VIBRATION SUPPRESSION

Dominik Niederberger ^{*,1} **Andrew Fleming** ^{**}
S. O. Reza Moheimani ^{**} **Manfred Morari** ^{*}

** Automatic Control Laboratory, Swiss Federal Institute of Technology,
Zurich, Switzerland.*

*** Laboratory for Dynamics and Control of Smart Structures, School of
Electrical and Computer Engineering, The University of Newcastle,
Australia.*

Abstract: Broadband structural vibration can be suppressed through the connection of an electrical impedance to the terminals of a bonded piezoelectric transducer. This is referred to as piezoelectric shunt damping. Good nominal damping performance has been obtained with resonant shunts, but these shunts are highly sensitive to variations in structural resonance frequencies. In this paper, we present an online tuned multi-mode resonant shunt controller. For optimal tuning, the parameters of this shunt are adjusted online by minimizing the relative phase difference between a vibration reference signal and the shunt current. Experiments validate the proposed technique and demonstrate the simplicity of implementation. The tuning law converges quickly and maintains optimal performance in the presence of environmental uncertainties.

Keywords: Active, Vibration, Control, Shunt, Damping, Adaptation

1. INTRODUCTION

Piezoelectric shunt damping is a popular technique for vibration suppression in smart structures. Techniques encompassed in this broad description are characterized by the connection of an electrical impedance to a structurally bonded piezoelectric transducer. Such methods do not require an external sensor, and may guarantee stability of the shunted system (Moheimani *et al.*, 2003). Piezoelectric shunt impedance designs have included resistors (Hagood and A. Von Flotow, 1991), inductive networks (Wu, 1996; Behrens *et al.*, 2002; Hollkamp, 1994), switched networks (Richard *et al.*, 2000; Corr and Clark, 2003), negative capacitors (Wu, 2000; Behrens *et al.*, 2003), and active impedances (Behrens *et al.*, 2003). Resonant shunt impedances (Wu, 1996; Behrens *et al.*, 2002) consisting of resistors, capacitors, and inductors are simple to

design and offer considerable effective modal damping. The performance of resonant shunt circuits is known to be highly sensitive to variations in the transducer capacitance and structural resonance frequencies (Hanselka, 2002; Niederberger *et al.*, 2003a). This paper introduces a new technique for the online tuning of multi-mode resonant piezoelectric shunt damping circuits.

Hollkamp (Hollkamp and T. F. Starchville, Jr., 1994) first demonstrated an adaptive single-mode shunt circuit by varying the value of a virtual inductor to minimize an RMS vibration signal. Virtual circuit implementations are complicated to construct, require a large number of high voltage components, and are generally unsuitable for damping more than two modes simultaneously. The synthetic impedance (Fleming *et al.*, 2002) was introduced as a simplified technique for the implementation of piezoelectric shunt impedances. A technique exploiting this flexibil-

¹ niederberger@control.ee.ethz.ch

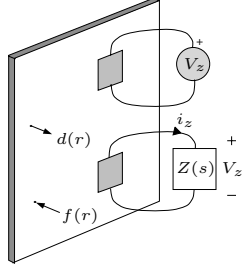


Figure 1. A general piezoelectric laminate structure excited by a point force $f(r, t)$, and the voltage V_a applied to a disturbance patch. The resulting vibration $d(r, t)$ is suppressed by the presence of an electrical impedance connected to the shunt transducer.

ity was presented in (Behrens *et al.*, 2002). A multi-mode circuit was tuned online to minimize an RMS strain signal estimated from the terminal voltage. Although this method requires no vibration sensor, it is slow to converge and is dependent on the disturbance spectrum.

A new adaptive technique based on relative phase shift was presented in (Niederberger *et al.*, 2003a). It was shown that minimizing the relative phase difference between a reference signal related to vibration and the shunt current, results in optimal tuning of the circuit parameters. This technique is not based on a time averaged RMS estimate and is thus faster to converge and displays significantly less mis-adjustment at the minima. In (Niederberger *et al.*, 2003a) a single-mode shunt circuit was implemented through the use of a variable virtual inductance. In this paper, the results are extended to multiple modes with the utilization of a synthetic impedance. The impedance dynamics and adaptation rule are computed in real time on a digital signal processor.

2. MODELING

Consider the piezoelectric laminate structure shown in Figure 1. The goal is to suppress vibration resulting from two disturbances: V_a , the voltage applied to a disturbance patch, and $f(r, t)$, a point force located at the point r .

For generality, the objective is to model the effect of a shunted piezoelectric transducer on the known model of a mechanical structure. The open-loop, i.e. with no shunt attached, transfer functions required are:

$$G_{va}(s) = \frac{V_p(s)}{V_a(s)}, G_{vv}(s) = \frac{V_p(s)}{V_z(s)} \text{ and } G_{da}(r, s) = \frac{d(r, s)}{V_a(s)}$$

where $V_p(s)$ is the piezoelectric voltage induced in the shunt transducer, and $d(r, s)$ is the displacement measured at a point r . If the disturbance and shunt transducer are identical, collocated, and poled in opposite directions like in Figure 2, $G_{va}(s) = -G_{vv}(s)$.

The above transfer functions can be derived analytically, for example by solving the Euler-Bernoulli beam equation (Fuller *et al.*, 1996). Alternatively,

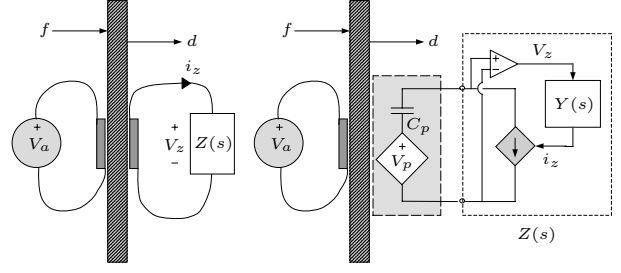


Figure 2. The physical and electrically equivalent view of a structure disturbed by an applied actuator voltage $V_a(s)$ and external force $F(r, s)$. The resulting vibration $d(r, s)$ is suppressed by the presence of a shunt impedance.

system identification (Ljung, 1999) can be employed to estimate these models directly from experimental data.

Following the modal analysis procedure (Meirovitch, 1996), the resulting transfer functions have the familiar form

$$G_{da}(r, s) = \frac{d(r, s)}{V_a(s)} = \sum_{k=1}^{\infty} \frac{F_k \phi_k(r)}{s^2 + 2\zeta_k \omega_k s + \omega_k^2}, \quad (1)$$

$$G_{vv}(s) = \frac{V_p(s)}{V_z(s)} = \sum_{k=1}^{\infty} \frac{\alpha_k}{s^2 + 2\zeta_k \omega_k s + \omega_k^2}, \quad (2)$$

where F_k , and α_k represent the lumped modal and piezoelectric constants applicable to the k^{th} mode of vibration.

2.1 Modeling the Presence of a Shunt Circuit

Using the open-loop transfer functions (1), the presence of an electrical impedance $Z(s)$ will now be incorporated into the structural dynamics. Referring to Figure 2, the relationship between voltage and current in the Laplace domain is

$$V_z(s) = I_z(s)Z(s). \quad (3)$$

Applying Kirchhoff's voltage law we obtain

$$V_z(s) = V_p(s) - \frac{1}{C_p s} I_z(s), \quad (4)$$

where C_p represents shunt transducer capacitance. Combining (3) and (4) we obtain

$$V_z(s) = \frac{C_p s Z(s)}{1 + C_p s Z(s)} V_p(s). \quad (5)$$

By applying the principle of superposition, the disturbance and shunt voltage strain contributions are

$$V_p(s) = G_{va}(s) V_a(s) + G_{vv}(s) V_z(s). \quad (6)$$

The shunted composite system can be obtained from Equations (3), (4), and (6),

$$\frac{V_p(s)}{V_a(s)} = \frac{G_{va}(s)}{1 + G_{vv}(s)K(s)}, \quad (7)$$

where

$$K(s) = \frac{-Z(s)}{Z(s) + \frac{1}{C_p s}}. \quad (8)$$

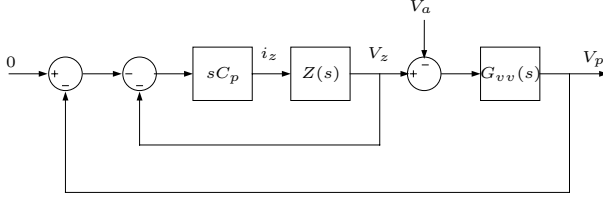


Figure 3. The strain-feedback interpretation of piezoelectric shunt damping with $G_{vv}(s) = -G_{va}(s)$.

The composite displacement transfer function can also be derived in a similar fashion,

$$\frac{d(r, s)}{V_a(s)} = \frac{G_{da}(r, s)}{1 + G_{vv}(s)K(s)}. \quad (9)$$

By again applying the principle of superposition, the effect of force disturbance $F(r, s)$ located at point r can be included,

$$V_p(s) = \frac{G_{va}(s)V_a(s)}{1 + G_{vv}(s)K(s)} + G_{vf}(r, s)F(r, s), \quad (10)$$

$$d(r, s) = \frac{G_{da}(r, s)V_a(s)}{1 + G_{vv}(s)K(s)} + G_{df}(r, s)F(r, s), \quad (11)$$

where $G_{df}(r, s)$ and $G_{vf}(r, s)$ are the respective transfer functions from an applied force $F(r, s)$ to the displacement $d(r, s)$ and shunt transducer piezoelectric voltage V_p , i.e.

$$G_{vf}(r, s) = \frac{V_p(s)}{F(r, s)} \quad G_{df}(r, s) = \frac{d(r, s)}{F(r, s)}. \quad (12)$$

From Equation (7) it can be concluded that the presence of an electrical shunt impedance parameterizes an equivalent collocated strain feedback controller. A diagrammatic representation of equation (7) is shown in Figure 3. Further interpretation and analysis can be found in (Moheimani *et al.*, 2003).

In section 4, where the experiments are presented, the transfer function $G_{\nu}(r, s)$ from an actuator disturbance voltage $V_a(s)$ to the velocity $\nu(r, s)$ is measured to validate the performance of the proposed shunt controllers. This transfer function is defined as

$$G_{\nu}(r, s) = \frac{\nu(r, s)}{V_a(s)} = sG_{da}(r, s). \quad (13)$$

3. ADAPTATION LAW

In this section, a new adaptation law for multi-mode resonant shunts is derived. First, the *relative phase adaptation* of single-mode $R - L$ shunts is reviewed, then extended to multi-mode resonant shunts.

3.1 Adaptive single-mode R-L Shunt

As shown in Section 2, an electrical shunt impedance parameterizes an equivalent collocated strain feedback controller. If the impedance $Z(s)$ is chosen as a series inductor-resistor network ($R - L$ shunt), a resonant

shunt controller is obtained that significantly reduces the vibration associated with a single structural mode (Hagood and A. Von Flotow, 1991). As described in (Hanselka, 2002; Niederberger *et al.*, 2003a), the damping performance of resonant shunts is sensitive to environmental variation in the structural resonance frequencies and transducer capacitance. Online tuning of the inductance L is required to maintain optimal damping. To this end, adaptive techniques based on Root Mean Square (RMS) minimization (Hollkamp and T. F. Starchville, Jr., 1994), and relative phase shift (Niederberger *et al.*, 2003a) have been proposed. These two approaches, applied to an electromagnetic system are compared in (Niederberger *et al.*, submitted 2003b). In that instance, relative phase adaptation tunes faster with less misadjustment than the *RMS* methodology. In the following, a review and extension of the relative phase adaptation is presented.

Relative phase adaptation is based on adjusting the relative phase difference between the velocity and shunt current to $-\pi/2$. A simple multiplication and filter operation evaluates the relative phase difference. Consider Figure 2, where $Z(s) = R + sL$. Inserting $V_z(s) = I_z(s) \cdot (R + sL)$ into Equation (5) leads to

$$I_z(s) = V_p(s) \frac{sC_p}{s^2LC_p + sC_pR + 1}. \quad (14)$$

As V_p is dynamically proportional to the strain $x(s)$ experienced by the piezoelectric transducer, i.e. $V_p(s) = cx(s) = c\nu(s)/s$, where c is a constant and $\nu(s)$ is the velocity, the transfer function $G_{I\nu}(s)$ from the velocity $\nu(s)$ to the current $I_z(s)$ can be expressed as

$$G_{I\nu}(s) = \frac{I_z(s)}{\nu(s)} = \frac{cC_p}{1 + sC_pR + s^2LC_p}. \quad (15)$$

The phase of $G_{I\nu}(j\omega)$ is

$$\angle(G_{I\nu}(j\omega)) = \phi_n = -\tan^{-1} \left(\frac{\omega C_p R}{1 - LC_p \omega^2} \right). \quad (16)$$

According to (Hagood and A. Von Flotow, 1991), optimal tuning of the $R - L$ shunt is achieved when $\omega_n = 1/(LC_p)$, where ω_n is the structural resonance frequency of the n th mode. From Equation 16, one can see that this tuning condition can be reformulated by the condition $\angle G_{I\nu}(j\omega_n) = -\pi/2$. A function $f_p(L, \omega_n) = \text{sign}(\angle(G_{I\nu}(j\omega_n)) + \frac{\pi}{2})$ can be defined that reveals the required tuning direction of the inductance value. The discrete adaptation of L that tunes the n th mode is given by

$$\begin{aligned} L_{k+1} &= L_k + \alpha \cdot \text{sign}(f_p(L_k, \omega_n)) \\ &= L_k + \alpha \cdot \text{sign} \left(\angle(G_{I\nu}(j\omega_n)) + \frac{\pi}{2} \right), \end{aligned} \quad (17)$$

where α is the tuning constant. A direct evaluation of the phase angle is not straight-forward and complicates the adaptation scheme shown above. A practical alternative for evaluating the tuning direction is shown in the following. If we assume that the velocity $\nu(t)$ and current $I_z(t)$ are tonal, a reasonable assumption

as the resonances are very lightly damped, the multiplication of $\nu(t) = \sin(\omega_n t)$ with $I_z(t)$ can be written as

$$\nu(t) \cdot I_z(t) = \sin(\omega_n t) \cdot A_n \sin(\omega_n t + \phi_n),$$

where ϕ_n is the phase shift equal to $\angle(G_{I\nu}(j\omega_n))$ and $A_n = |G_{I\nu}(j\omega_n)|$. After some manipulations, the following expression can be obtained

$$\nu(t) \cdot I_z(t) = A_n \left(\frac{1}{2} (\cos(\phi_n) - \cos(2\omega_n t + \phi_n)) \right). \quad (18)$$

By low-pass filtering the above expression with a cut-off frequency below $2\omega_n$, the second term can be neglected and one gets

$$g_{LP}(t) * [\nu(t) \cdot I_z(t)] = \frac{A_n}{2} \cdot \cos(\phi_n), \quad (19)$$

where $g_{LP}(t)$ represents the impulse response of a low-pass filter, and $*$ denotes the time domain convolution operator. It can be seen that

$$\begin{aligned} \text{sign}(g_{LP}(t) * [\nu(t) \cdot I_z(t)]) &= \text{sign}(\cos(\phi_n)) \\ &= \text{sign}\left(\angle(G_{I\nu}(j\omega_n)) + \frac{\pi}{2}\right), \end{aligned} \quad (20)$$

for $-\frac{3\pi}{2} < \phi_n < \frac{\pi}{2}$. This technique constitutes a new means for evaluating the tuning direction. The discrete adaptation law can be rewritten as

$$L_{k+1} = L_k + \alpha \cdot \text{sign}(g_{LP}(t) * [\nu(t) \cdot I_z(t)]). \quad (21)$$

By removing the sign operator, effectively allowing the tuning rate to vary, the following continuous tuning law can be obtained

$$\frac{dL(t)}{dt} = \beta (g_{LP}(t) * [\nu(t) \cdot I_z(t)]), \quad (22)$$

where β is the tuning rate. Equation 22 represents the proposed relative phase adaptation law for single-mode $R - L$ shunts.

3.2 Adaptive Resonant Multi-Mode Shunts

Multi-mode shunt damping techniques were introduced to allow the control of multiple structural modes with a single piezoelectric transducer. (Wu, 1996) proposed the so-called current-blocking techniques where a parallel capacitor and inductor are inserted in series with each single-mode shunt branch. One associated problem is the required circuit size to damp 3 or more modes, the order of the shunt circuit increases quadratically as the number of modes to be damped increases. Current-flowing circuits (Behrens *et al.*, 2002), such as that pictured in Figure 4, are easier to tune and increase only linearly in order as a greater number of modes are to be shunt damped simultaneously. At a specific frequency ω_i , the inductor capacitor network $C_{Fi} - L_{Fi}$ allows current to flow through the rest of the branch, at all other frequencies the branch appears

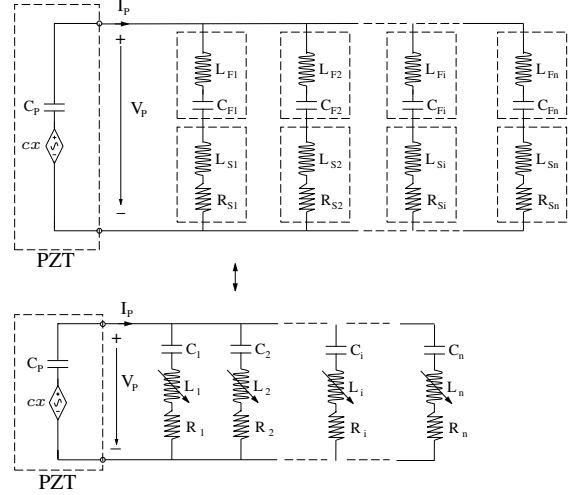


Figure 4. Current-flowing circuit and its simplification

approximately as an open circuit. The damping inductor and resistor $L_{Si} - R_{Si}$ acts analogous to a single-mode shunt circuit at the frequency ω_i . The circuit is simplified by combining the series inductors L_{Fi} and L_{Si} to L_i (Figure 4 bottom).

In the following, the inductive elements in a current-flowing circuit will be adapted online to compensate for variation in structural resonance frequencies and transducer capacitance. In previous multi-mode techniques, the inductors have been tuned by minimizing a signal related to the *RMS* strain (Fleming and Moheimani, 2003a). The branch inductor values were updated using a gradient search algorithm. As the performance function is rather flat around the optimum, this strategy is slow to converge and is prone to misadjustment after the minimum has been reached. A new technique based on relative phase adaptation will now be presented.

First, due to the series $C_{Fi} - L_{Fi}$ network, we notice that each branch can be regarded independently. The series $C_{Fi} - L_{Fi}$ network has zero impedance for $\omega = \frac{1}{\sqrt{C_{Fi}L_{Fi}}}$ and has high impedance at all other frequencies. Therefore, the transfer function from structural velocity to the current I_i in the i th branch can be written around the i th modal resonance frequency ($s \approx j\omega_i$) as

$$G_i(s) = \frac{I_n(s)}{\nu(s)} = \frac{c}{s} \cdot \frac{s/L_i}{s^2 + s \frac{R_i}{L_i} + \frac{C_i + C_p}{C_p C_i L_i}}, \quad (23)$$

where the electrical resonance frequency is

$$\omega_{iel}^2 = \frac{C_i + C_p}{C_i C_p L_i} = \frac{1}{L_i C_{eqi}}. \quad (24)$$

The phase of $G_i(j\omega)$ becomes

$$\angle(G_i(j\omega)) = -\tan^{-1} \left(\frac{\omega R_i / (L_i)}{(C_i + C_p) / (C_i C_p L_i) - \omega^2} \right)$$

and is $-\pi/2$ for $\omega_i = 1/\sqrt{C_{eqi}L_i}$ with $C_{eqi} = (C_i + C_p)/(C_i C_p)$. Thus we can use relative phase

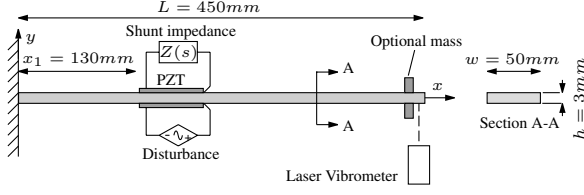


Figure 5. Experimental piezoelectric laminated cantilever structure.

adaptation to tune the i th branch to the corresponding mechanical mode. As the branches naturally bandpass filter the current at the corresponding resonance frequency, no additional bandpass filters for the current signal are necessary. Velocity bandpass filters are not required either as long as the mechanical resonance frequencies are not harmonic. The adaptation of the inductor vector $\bar{L}(s)$ is

$$\frac{\partial \bar{L}(s)}{\partial t} = \begin{pmatrix} \dot{L}_1(t) \\ \dot{L}_2(t) \\ \vdots \\ \dot{L}_n(t) \end{pmatrix} = \begin{pmatrix} \alpha_1 \cdot g_{LP}^1(t) * [\nu(t) \cdot I_1(t)] \\ \alpha_2 \cdot g_{LP}^2(t) * [\nu(t) \cdot I_2(t)] \\ \vdots \\ \alpha_n \cdot g_{LP}^n(t) * [\nu(t) \cdot I_n(t)] \end{pmatrix}$$

where α_i is the i^{th} tuning rate, and $g_{LP}^i(t)$ is the i th low-pass filter with a cut-off frequency below $2\omega_i$.

4. EXPERIMENTS

In this section, relative phase adaptation is used to tune and maintain the optimal performance of a two mode resonant shunt damping circuit. The experiments were carried out on a cantilevered piezoelectric laminate beam at the Laboratory for Dynamics and Control of Smart Structures, University of Newcastle, Australia.

4.1 Synthetic Impedance

As shown in Figure 2, an arbitrary impedance can be implemented with a voltage measurement, signal filter, and current source. A dSpace 1005 system was used to implement all of the filtering and processing tasks. More details on the construction of the electronics can be found in (Fleming and Moheimani, 2003b).

4.2 Damping of a Piezoelectric Laminated Beam

The experimental structure is a uniform aluminum beam with rectangular cross-section. The set-up is displayed in Figure 5. Two identical piezoelectric patches are laminated symmetrically onto the front and back faces of the beam. One patch generates strain disturbance in the beam. The adaptive shunt impedance is connected to the other patch.

The second and third modes of the cantilever beam are damped using the online-tuned multi-mode resonant shunt. We examine the behavior of the adaptive shunt

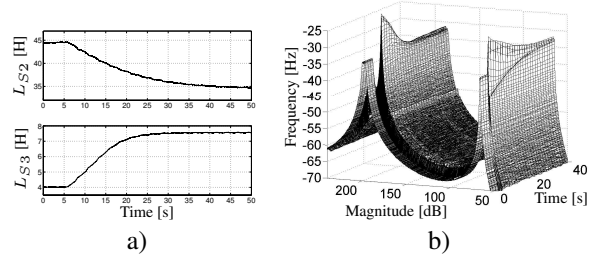


Figure 6. a) Time evolution of the inductance values L_{S2} and L_{S3} after a step change in the resonance frequencies. b) Magnitude of $G_\nu(s)$ as a function of time, after a change in the resonance frequencies.

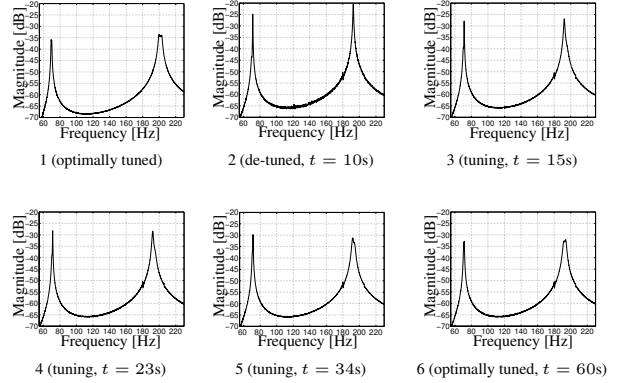


Figure 7. Magnitude of the transfer functions $G_\nu(r, s)$ during adaptation. At time $t = 10$ s, the modal frequency changes. In the following plots 3 to 6, the relative phase adaptation is re-tuning until the optima is reached again in plot 6.

subject to a step change in the structural resonance frequencies. The modal frequencies are disturbed by attaching an additional mass to the cantilever beam. The second mode moves from 69.5 Hz to 71.2 Hz, and the third mode from 201.2 Hz to 192.6 Hz. In Figure 7-1, the multi-mode shunt is optimally tuned and the corresponding inductances are $L_{S2} = 44.5$ H and $L_{S3} = 4$ H (see Figure 6 a). The additional mass is then attached effectively detuning the multi-mode shunt. In the following plots 3 to 6 of Figure 7, the relative phase adaptation is re-tuning until the optima is reached again in plot 6. The tuning behavior can also be observed in Figure 6 a) where the initial inductances are $L_{S2} = 44.5$ H and $L_{S3} = 4$ H (optimal). After the additional mass is attached, the inductance values tune to $L_{S2} = 34.5$ H and $L_{S3} = 7.5$ H. The evolution of the magnitude transfer-function $G_\nu(r, s)$ during adaptation is shown in Figure 6 b).

4.2.1. Sensitivity Analysis This section analyzes the sensitivity of the tuning law. Figure 8 a) shows the tuning direction of L_{S2} , i.e. $\text{sign}(g_{LP}^2(t) * [I_2(t) \cdot \nu(t)])$, as a function of L_{S2} and L_{S3} . As desired, the tuning direction is dependent only on L_{S2} . The tuning direction of L_{S3} is shown in Figure 8 b) and it is dependent only on L_{S3} . From these plots we can ascertain that there is no cross correlation between the tuning of L_{S2} and L_{S3} , and that each current-flowing branch operates independently over the range examined.

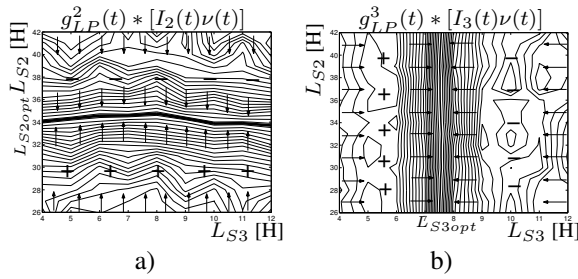


Figure 8. Measured tuning direction a) $dL_{S2}(L_{S2}, L_{S3})$ and b) $dL_{S3}(L_{S2}, L_{S3})$, i.e. $\text{sign}(g_{LP}^2(t) * [I_2(t)\nu(t)])$ and $\text{sign}(g_{LP}^3(t) * [I_3(t)\nu(t)])$.

5. CONCLUSION

Standard multi-mode resonant shunts are known to be highly sensitive to variations in the transducer capacitance and structural resonance frequencies. In many practical applications, such shunt circuits require on-line component value optimization.

Former adaptive techniques based on RMS minimization require excessively long convergence times and are prone to misadjustment. In this paper, a new technique has been introduced for the online tuning of resonant piezoelectric shunt damping circuits. The tuning law is based on minimizing the relative phase difference between a vibration reference signal and the shunt branch current.

Experiments have demonstrated the adaptive shunt damping of two structural modes simultaneously. Optimal performance was maintained in the presence of artificial variations in structural resonance frequency. The technique is easy to implement, requires little additional computation or electronics, and is suitable for practical applications.

ACKNOWLEDGMENTS

Support for this research has been provided by grants from ETH (Zurich), EMPA (Dübendorf) and ARC (Australia). The experimental facilities were provided by the Laboratory for Dynamics and Control of Smart Structures (LDCSS).

6. REFERENCES

Behrens, S., A. J. Fleming and S. O. R. Moheimani (2003). A broadband controller for shunt piezoelectric damping of structural vibration. *Smart Materials and Structures* **12**, 18–28.

Behrens, S., S. O. R. Moheimani and A. J. Fleming (2002). Multiple mode passive piezoelectric shunt dampener. In: *Proc. IFAC Mechatronics 2002*. Berkeley, CA.

Corr, L. R. and W. W. Clark (2003). A novel semi-active multi-modal vibration control law for a piezoceramic actuator. *Journal of Vibration and Acoustics, Transactions of the ASME*.

Fleming, A. J. and S. O. R. Moheimani (2003a). Adaptive piezoelectric shunt damping. *Smart Materials and Structures* **12**, 36–48.

Fleming, A. J. and S. O. R. Moheimani (2003b). Improved current and charge amplifiers for driving piezoelectric loads. In: *Proc. SPIE Smart Structure and Materials, Vol.5052*.

Fleming, A. J., S. Behrens and S. O. R. Moheimani (2002). Optimization and implementation of multi-mode piezoelectric shunt damping systems. *IEEE/ASME Transactions on Mechatronics* **7**(1), 87–94.

Fuller, C. R., S. J. Elliott and P. A. Nelson (1996). *Active Control of Vibration*. Academic Press.

Hagood, N. W. and A. Von Flotow (1991). Damping of structural vibrations with piezoelectric materials and passive electrical networks. *Journal of Sound and Vibration* **146**(2), 243–268.

Hanselka, H. (2002). Adaptronik und Fragen zur Systemzuverlässigkeit. *ATP, Automatisierungstechnische Praxis* **2**, 44–49.

Hollkamp, J. J. (1994). Multimodal passive vibration suppression with piezoelectric materials and resonant shunts. *Journal of Intelligent Materials Systems and Structures* **5**, 49–56.

Hollkamp, J. J. and T. F. Starchville, Jr. (1994). A self-tuning piezoelectric vibration absorber. *Journal of Intelligent Material Systems and Structures* **5**, 559–565.

Ljung, L. (1999). *System Identification: Theory for the User*. Prentice Hall.

Meirovitch, L. (1996). *Elements of Vibration Analysis*. 2nd ed.. McGraw-Hill. Sydney.

Moheimani, S. O. R., A. J. Fleming and S. Behrens (2003). On the feedback structure of wideband piezoelectric shunt damping systems. *Smart Materials and Structures* **12**, 49–56.

Niederberger, D., M. Morari and S. Pietrzko (2003a). Adaptive resonant shunted piezoelectric devices for vibration suppression. In: *Proc. SPIE Smart Structures and Materials, Vol.5056*. pp. 213–224.

Niederberger, D., S. Behrens, A. J. Fleming, S. O. R. Moheimani and M. Morari (submitted 2003b). Adaptive electromagnetic system for shunt damping. *IEEE/ASME Transactions on Mechatronics*.

Richard, C., D. Guyomar, D. Audigier and H. Bassaler (2000). Enhanced semi-passive damping using continuous switching of a piezoelectric devices on an inductor. In: *Proc. SPIE Smart Structures and Materials, Damping and Isolation, Vol.3989*. pp. 288–299.

Wu, S. Y. (1996). Piezoelectric shunts with parallel R-L circuit for structural damping and vibration control. In: *Proc. SPIE Smart Structures and Materials, Vol.2720*. pp. 259–269.

Wu, S. Y. (2000). Broadband piezoelectric shunts for structural vibration control. Patent No. 6,075,309.